

# Natural convection boundary layer along impermeable inclined surfaces embedded in porous medium

M. H. Kayhani\*, E. Khaje\*\*, M. Sadi\*\*\*

\*Mechanical Department, Shahrood University of technology, Shahrood, Iran, E-mail: m\_kayhani@yahoo.com

\*\*Mechanical Department, Shahrood University of technology, Shahrood, Iran, E-mail: esmaeilkhaje@yahoo.com

\*\*\*Mechanical Department, Shahrood University of technology, Shahrood, Iran, E-mail: meisam.sadi@gmail.com

crossref <http://dx.doi.org/10.5755/j01.mech.17.1.205>

## 1. Introduction

Convection heat transfer in a saturated porous medium is in great attention for many applications in geophysics and energy systems. Applications such as geothermal energy utilization, ground water pollution analysis, insulation of buildings, paper production and petroleum reservoir can be cited. These applications have been widely discussed in recent books by Nield and Bejan [1], Ingham and Pop [2], Vafai [3], Pop and Ingham [4] and Ingham et al. [5]. However, natural convection along inclined plates has received less attention than the cases of vertical and horizontal plates. Rees and Riley [6], and Ingham et al. [7] presented some solution for free convection along a flat plate in a porous medium which are only valid at small angles to the horizon. Jang and Chang [8] studied free convection on an inclined plate with power function distribution of wall temperature, while its angle varies between 0 to close to 90 degrees from horizontal. While Pop and Na [9] have solved the free convection of an isothermal inclined surface. Their solution included all horizontal to vertical cases. Hossain and Pop [10] studied the effect of radiation. Conjugate convection from a slightly inclined plate was studied analytically and numerically by Vaszi et al. [11]. Lesnic et al. [12] studied analytically and numerically the case of a thermal boundary condition of mixed type on a nearly horizontal surface.

The purpose of this paper is to study natural convection above an inclined flat plate at a variable temperature range embedded in saturated porous medium. There is power-law variation in the wall temperature.

Coordinate system introduced by Pop and Na [9] is used in the solution. Then the system of two equations can be solved by finite difference technique proposed by Keller [13] for both the cases of positively inclined plate ( $0^\circ \leq \phi \leq 90^\circ$ ) and negatively inclined plate at small angles to the horizontal ( $\phi \leq 0^\circ$ ). The effect of inclination parameter on skin friction coefficient and Nusselt number and also the dimensionless velocity and temperature profiles have been investigated. However, the free convection has been solved on the horizontal and vertical plates earlier by Cheng and Chang [14], and Cheng and Minkowycz [15] respectively.

## 2. Governing equations

Consider the steady natural convection from an arbitrarily inclined plate embedded in an isothermal porous medium at temperature  $T_\infty$ . Assume that the wall tempera-

ture is kept at a higher value with the power-law variation. The inclination angle is either positive ( $0^\circ \leq \phi \leq 90^\circ$ ) or slightly negative ( $\phi \leq 0^\circ$ ). The physical model and coordinate system is given in Fig. 1. Here  $(x, y)$  are Cartesian coordinates along and normal to the plate, with positive  $y$  axis pointing toward the porous medium.

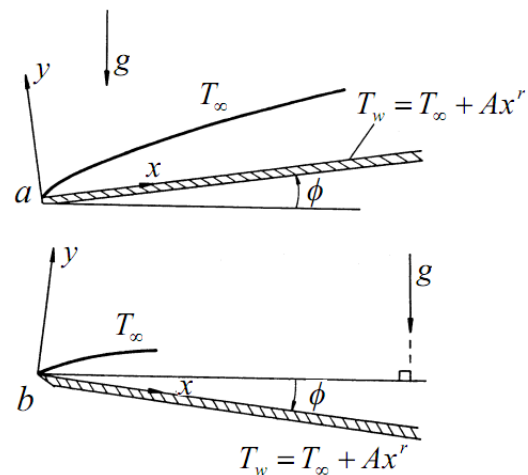


Fig. 1 Physical model and coordinate system: a - positive inclination; b - negative inclination

If the following assumptions have been used (i) the convective fluid and the porous medium are in thermodynamic equilibrium anywhere, (ii) the temperature of the fluid is below boiling point at any point of domain, (iii) the fluid and porous medium properties are constant except the variation of fluid density with temperature, and (iv) the Darcy-Boussinesq approximation is employed, the velocity and temperature within the momentum and thermal boundary layers which develop along the inclined plate are governed by the following equations:

$$\frac{\partial u}{\partial x} + \frac{\partial v}{\partial y} = 0 \quad (1)$$

$$u = -\frac{K}{\mu} \left( \frac{\partial p}{\partial x} \pm \rho g \sin \phi \right) \quad (2)$$

$$v = -\frac{K}{\mu} \left( \frac{\partial p}{\partial y} + \rho g \cos \phi \right) \quad (3)$$

$$u \frac{\partial T}{\partial x} + v \frac{\partial T}{\partial y} = \alpha \left( \frac{\partial^2 T}{\partial x^2} + \frac{\partial^2 T}{\partial y^2} \right) \quad (4)$$

$$\rho = \rho_\infty [1 - \beta (T - T_\infty)] \quad (5)$$

where the “+” and “-” signs in Eq. (2) indicate the positive and negative inclinations of the plate respectively. Here in Eqs. (1)-(5)  $u$ ,  $v$  are the velocity components along  $(x, y)$  axes;  $K$  is the permeability of porous medium;  $\mu$ ,  $\rho$ ,  $\beta$  and  $\alpha$  are the viscosity, density, coefficient of thermal expansion and thermal diffusivity, respectively;  $T$ ,  $p$ ,  $g$  are also temperature, pressure and gravity acceleration. The subtitle “ $\infty$ ” also refers to conditions in the infinite distance. Boundary conditions of the problem are as

$$v = 0, \quad T = T_w = T_\infty + Ax^r \quad \text{on } y = 0 \quad (6)$$

$$u = 0, \quad T = T_\infty \quad \text{as } y \rightarrow \infty \quad (7)$$

By deriving Eqs. (2) and (3), respect to  $y$  and  $x$  respectively and applying Darcy-Boussinesq approximation and considering boundary layer approximations, Eqs. (8) and (9) are derived and with continuity equation form governing equations of the problem are as below

$$\frac{\partial u}{\partial y} = \frac{gK\beta}{\nu} \left( \pm \frac{\partial T}{\partial y} \sin \phi - \frac{\partial T}{\partial x} \cos \phi \right) \quad (8)$$

$$u \frac{\partial T}{\partial x} + v \frac{\partial T}{\partial y} = \alpha \frac{\partial^2 T}{\partial y^2} \quad (9)$$

To convert Eqs. (1), (8) and (9) to the equations that could describe natural convection flow from an arbitrarily inclined plate in a porous medium, the parameter which was introduced by Pop and Na [9], is used

$$\xi = \frac{(Ra |\sin \phi|)^{1/2}}{(Ra \cos \phi)^{1/3}} \quad (10)$$

where  $Ra = gK\beta(T_w - T_\infty)x / \alpha\nu$  is the Rayleigh number. This parameter describes the relative strength of the longitudinal to the normal components of the buoyancy force that simultaneously applies on the boundary layer. Also for a fixed inclination angle, it could be used as a longitudinal coordinate. In addition, the forward variables are used.

$$\xi = \frac{\zeta}{1+\zeta}, \quad \eta = \left( \frac{y}{x} \right) \lambda \quad (11)$$

where

$$\lambda = (Ra \cos \phi)^{1/3} + (Ra |\sin \phi|)^{1/2} \quad (12)$$

Because at a given  $\phi$ ,  $\xi$  is defined as  $\xi = 1 / (1 + \text{constant} \cdot x^{-(r+1)/6})$ , this parameter shows the distance from the leading edge for a particular inclination angle. In addition  $\xi$ , changes from 0 to 1 as an inclination parameter at a fixed Rayleigh number by changing the angle  $\phi$  from  $0^\circ$  to  $90^\circ$ . Now it is possible to define the reduced stream function and dimensionless temperature as following

$$f(\xi, \eta) = \frac{\psi}{\alpha\lambda}, \quad \theta(\xi, \eta) = \frac{T - T_\infty}{T_w - T_\infty} \quad (13)$$

where  $\psi$  is the stream function and defined as

$$u = \frac{\partial \psi}{\partial y}, \quad v = -\frac{\partial \psi}{\partial x} \quad (14)$$

Based on the new variables, new equations are as following

$$f'' + (1-\xi)^3 \left\{ r\theta + \eta\theta' \left[ \frac{r+1}{6}(2+\xi) - 1 \right] \right\} = \pm \xi^2 \theta' - \left( \frac{r+1}{6} \right) \xi (1-\xi)^4 \frac{\partial \theta}{\partial \xi} \quad (15)$$

$$\theta'' + \frac{r+1}{6} (2+\xi) f\theta' - rf'\theta = \left( \frac{r+1}{6} \right) \xi (1-\xi) \left( f' \frac{\partial \theta}{\partial \xi} - \theta' \frac{\partial f}{\partial \xi} \right) \quad (16)$$

These equations should satisfy the following boundary conditions.

$$f = 0, \quad \theta = 1 \quad \text{on } \eta = 0 \quad (17)$$

$$f' = 0, \quad \theta = 0 \quad \text{as } \eta \rightarrow \infty \quad (18)$$

Primes show differentiation with respect to  $\eta$ . As obvious to solve Eqs. (15) and (16), having an initial condition for  $\xi$  is necessary. This condition is obtained by the solution of the equations for horizontal plate with  $\phi = 0^\circ$  and  $\xi = 0$ . Also, at  $\xi = 0$  or  $\phi = 0^\circ$ , Eqs. (15) and (16) declined to the equations of horizontal flat plate embedded in porous medium which presented by Cheng and Chang [14]

$$f'' + r\theta + \frac{r-2}{3} \eta\theta' = 0 \quad (19)$$

$$\theta'' + \frac{r+1}{3} f\theta' - rf'\theta = 0 \quad (20)$$

For the case  $\xi = 1$  or  $\phi = 90^\circ$ , the equations change to the equations expressed by Cheng and Minkowycz [15] for a vertical plate

$$f'' = \theta' \quad (21)$$

$$\theta'' + \frac{r+1}{2} f\theta' - rf'\theta = 0 \quad (22)$$

Quantities such as skin friction coefficient and Nusselt number can now be defined as following and investigated

$$C_f = \frac{\tau_w}{\rho U_c^2}, \quad Nu = \frac{xq_w}{k(T_w - T_\infty)} \quad (23)$$

where  $U_c = (\alpha\nu/x^2)^{1/2}$  is characteristic velocity,  $\tau_w$  is skin friction and  $q_w$  is heat flux at the wall which are normally given as

$$\tau_w = \mu \left( \frac{\partial u}{\partial y} \right)_{y=0}, \quad q_w = -k \left( \frac{\partial T}{\partial y} \right)_{y=0} \quad (24)$$

where  $k$  is thermal conductivity of the porous medium. By using Eqs. (11) and (13)

$$\frac{C_f}{(Ra \cos \phi)} = (1+\zeta)^3 f''(\xi, 0) \quad (25)$$

$$\frac{Nu}{(Ra \cos \phi)^{1/3}} = (1+\zeta) [-\theta'(\xi, 0)]. \quad (26)$$

### 3. Results and discussions

The coupled differential equations of Eqs. (15) and (16) are solved under boundary condition Eqs. (17) and (18) by Keller numerical scheme [13]. Based on  $\xi$  definition, numerical solution is started in  $\xi = 0$  and it continues step by step to  $\xi = 1$ . To start numerical solution, similarity solutions of free convection along horizontal flat plate presented in Eqs. (19) and (20) are used.

Solution of the equations is implemented for  $0 \leq r \leq 1$  which is available for both vertical and horizontal cases. For validating calculations, vertical solution results of Cheng and Minkowycz [15] are used. For further information on the numerical solution, it could be referred to [16].

*Positive inclination.* Figs. 2 and 3 depict skin friction coefficient and Nusselt number versus  $\xi$  for different values of  $r$ . Table presents results of similarity solution of Eqs. (21) and (22) and numerical solution at  $\xi = 1$  or  $\phi = 90^\circ$ . There is an excellent agreement between the results. As it can be seen, in a state of constant temperature, absolute value of skin friction coefficient is strictly ascending with increasing angle. This is due to the increase of buoyancy force in tangent direction of the plate. But in other cases, wall temperature changes also effect on the problem and cause changes to the diagram pattern. More

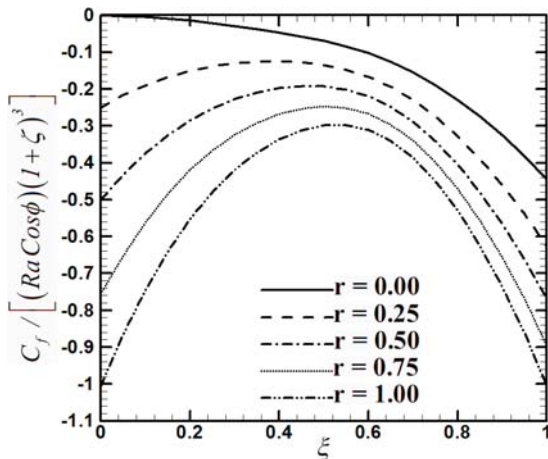


Fig. 2 Variation of the skin friction coefficient with  $\xi$  for positive inclination

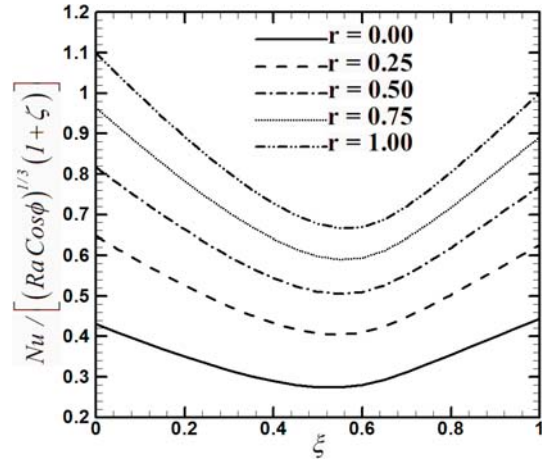


Fig. 3 Variation of the Nusselt number with  $\xi$  for positive inclination

over, by increasing  $r$ , absolute value of skin friction coefficient increases in the constant inclination angle. The reason is the increment of buoyancy force which induced due to temperature difference. Nusselt number increases with increasing  $r$ . In addition, in all cases by increasing  $\xi$ , Nusselt number declines at first and at  $\xi \approx 0.55$  where the tangential and normal components of buoyancy force are comparable, achieve to minimum, then again it moves upward.

Table

Comparison between values of  $-\theta'(0)$  from Cheng and Minkowycz [11] and present results at  $\xi = 1$

$r$	Cheng and Minkowycz [11]	Present results
0	0.444	0.444
0.25	0.630	0.627
0.5	0.761	0.764
0.75	0.892	0.892
1	1.001	1

Dimensionless velocity and temperature profiles have been plotted in Figs. 4-9 for different  $r$  and  $\xi$ . Profiles related to the horizontal and vertical plates that have good agreement with similarity solution are also given.

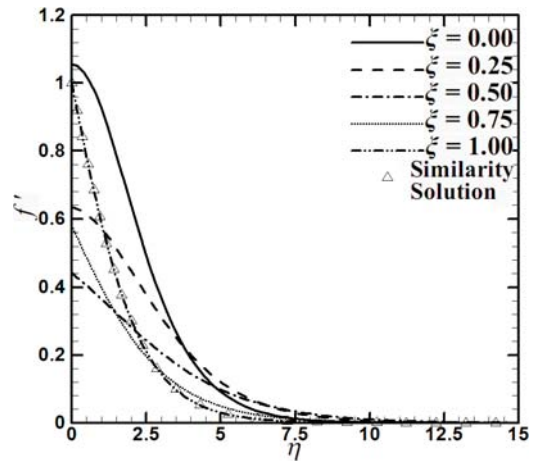


Fig. 4 Dimensionless velocity profiles for  $r = 0.00$  in positive inclination case

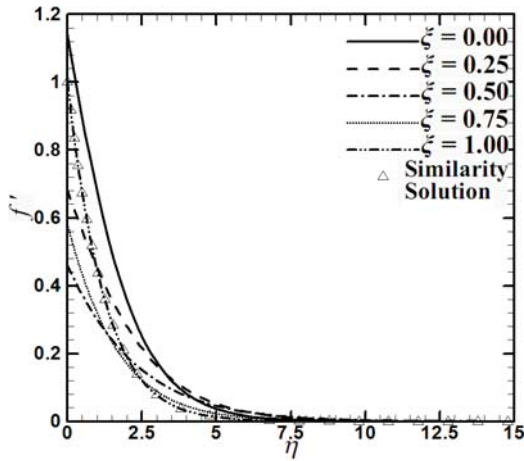


Fig. 5 Dimensionless velocity profiles for  $r = 0.50$  in positive inclination case

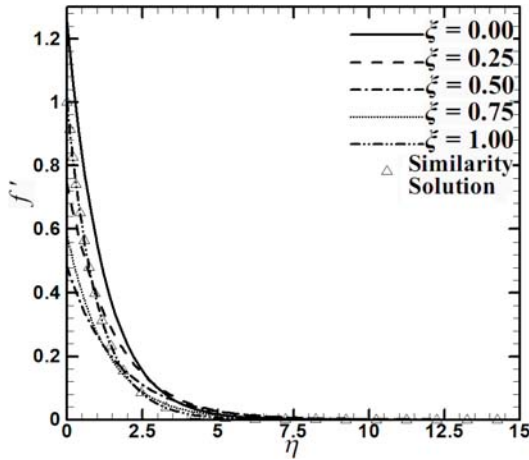


Fig. 6 Dimensionless velocity profiles for  $r = 1.00$  in positive inclination case

As it could be seen in Figs. 4-6, for a given  $\xi$ , by the increment of  $r$ , the slope of dimensionless velocity profiles increases and causes the increase in skin friction coefficient. Moreover in all cases except  $\xi = 1$ , this increment causes the increase in dimensionless velocity. This is because the tangential component of buoyancy force increases.

Figs. 7-9 depict that the slope of dimensionless temperature profiles increases by increasing  $r$  for a given  $\xi$ , which validated the increment of Nusselt number. For all  $\xi$ , by increasing  $r$  the decrease in momentum and thermal boundary layer thicknesses is visible.

*Negative inclination.* It is expected that for negative inclinations, the boundary layer separates with the increase in distance from leading edge, because the buoyancy force is exerted to the top of surface and causes the flow to return. When the plate velocity reaches negative values, the fluid starts to move upward and causing boundary layer separation occurs. Thus boundary layer equations have been broken before separation point and in general a new scaling is necessary in separation region. So that the  $\xi$  in which boundary layer equations are broken is only an estimate of the separation point and therefore  $(\xi_s)_{approx}$  is specified. From the solution of equations  $(\xi_s)_{approx} \approx 0.67$  is achieved. The solution does not converge for the values higher than that.

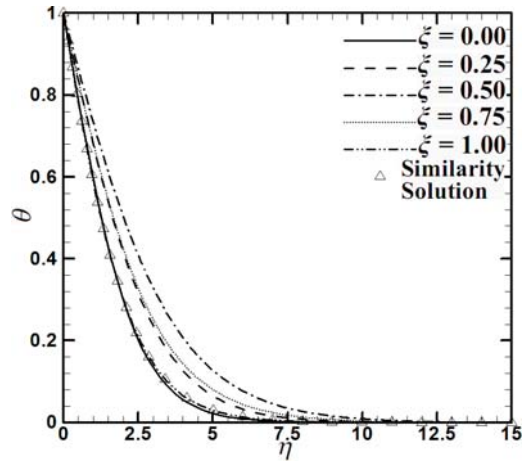


Fig. 7 Dimensionless temperature profiles for  $r = 0.00$  in positive inclination case

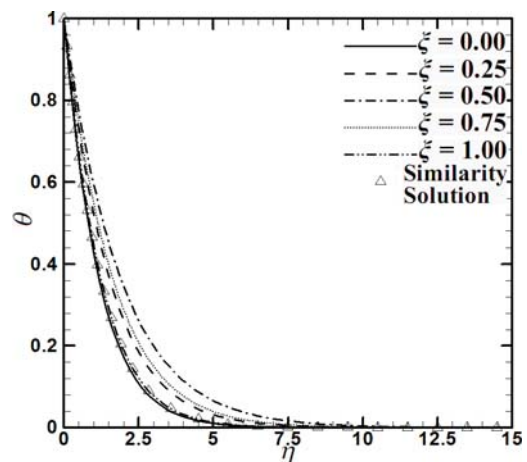


Fig. 8 Dimensionless temperature profiles for  $r = 0.50$  in positive inclination case

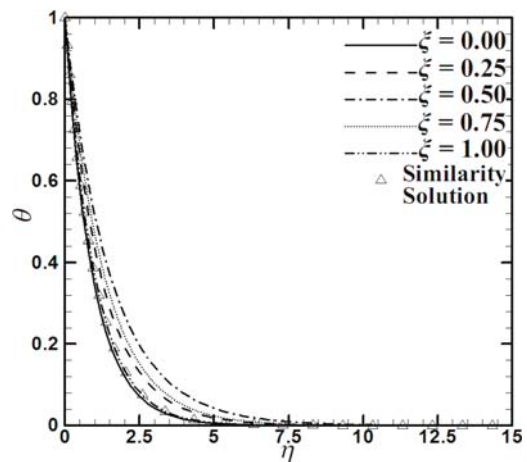


Fig. 9 Dimensionless temperature profiles for  $r = 1.00$  in positive inclination case

Due to the previous description, the variations of skin friction coefficient and Nusselt number for negative inclination angles are presented in Figs. 10 and 11 respectively. Again in this case at certain  $\xi$  an increase in  $r$  increases skin friction coefficient and the Nusselt number.

At the end, the dimensionless velocity and temperature profiles are depicted for different values of  $r$  and  $\xi = 0, 0.25$  and  $0.5$  in Figs. 12-17.



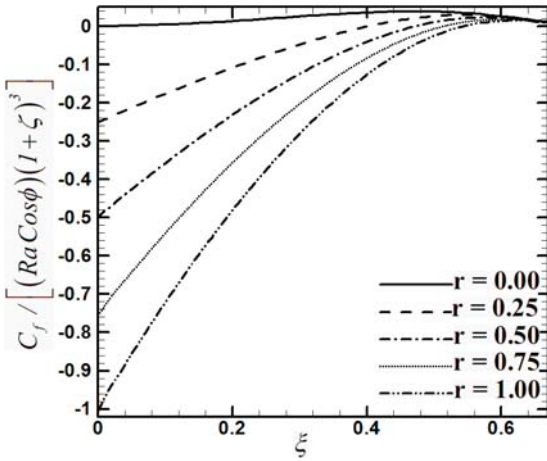


Fig. 10 Variation of the skin friction coefficient with  $\xi$  for negative inclination

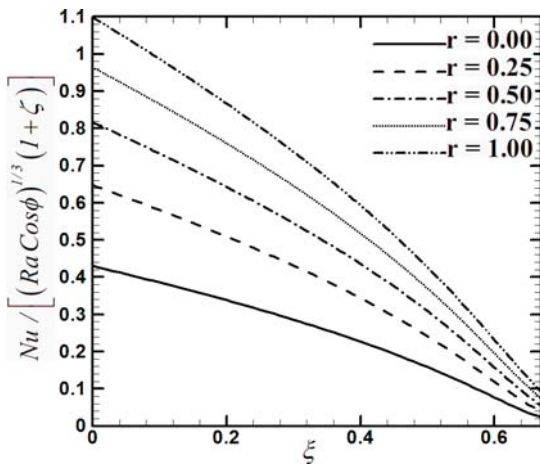


Fig. 11 Variation of the Nusselt number with  $\xi$  for negative inclination

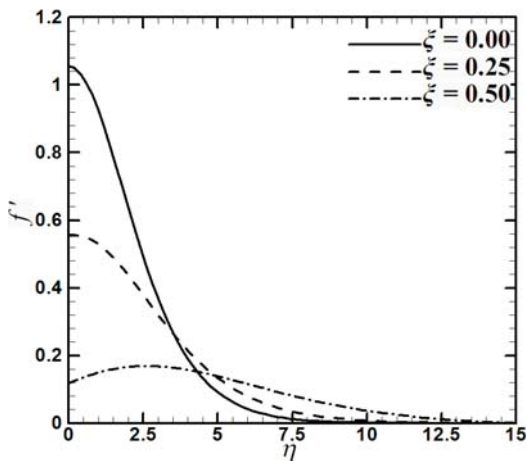


Fig. 12 Dimensionless velocity profiles for  $r = 0.00$  in negative inclination case

As it observed from Figs. 12-14, at a given  $r$  for smaller values of  $\xi$  dimensionless velocity profiles have steeper slope, on the other hand, increasing  $r$  at a given  $\xi$  increases profile slope. The skin friction coefficient variations graph also confirms these results. For  $\xi = 0.50$  the

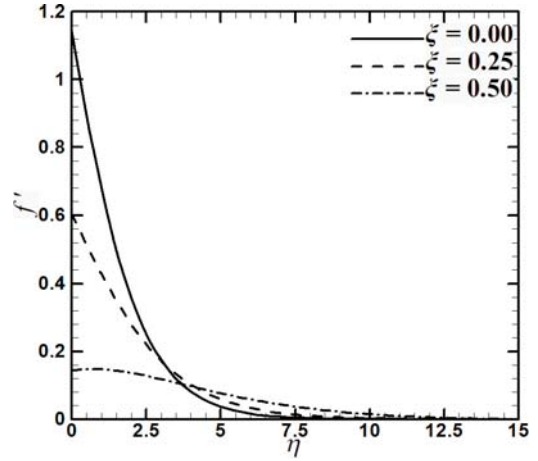


Fig. 13 Dimensionless velocity profiles for  $r = 0.50$  in negative inclination case

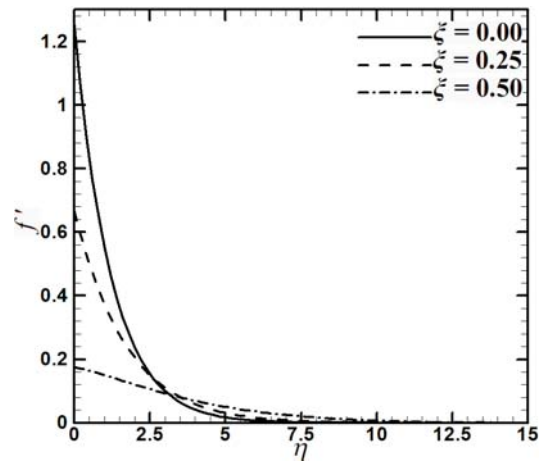


Fig. 14 Dimensionless velocity profiles for  $r = 1.00$  in negative inclination case

boundary layer thickness is higher than in the other cases, due to the approach of separation point.

Figs. 15-17 show that with increasing  $\xi$  in a certain  $r$ , the slope of temperature profiles decreases, which reflects the Nusselt number reduction. It is also approved by Fig. 11. On the other hand the temperature profiles increase with the increase in  $\xi$  at a given  $r$ .

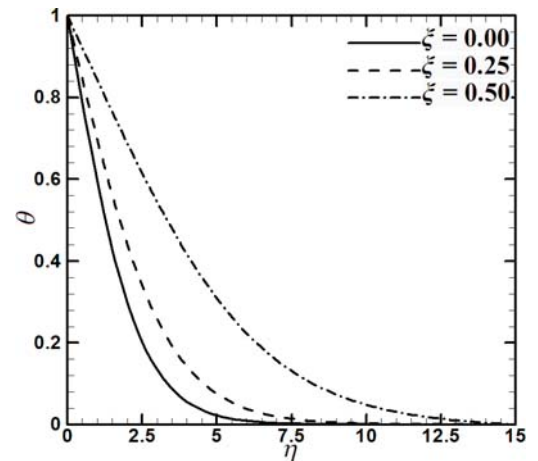


Fig. 15 Dimensionless temperature profiles for  $r = 0.00$  in negative inclination case

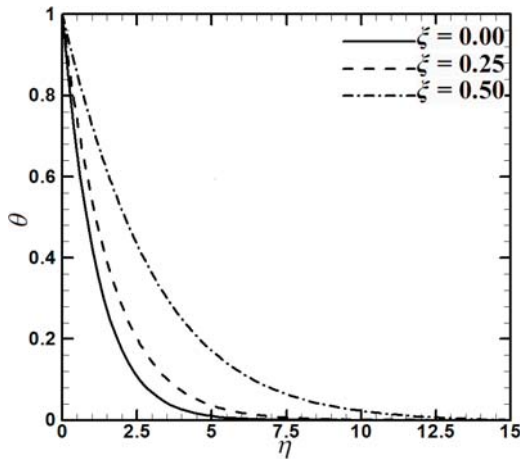


Fig. 16 Dimensionless temperature profiles for  $r = 0.50$  in negative inclination case

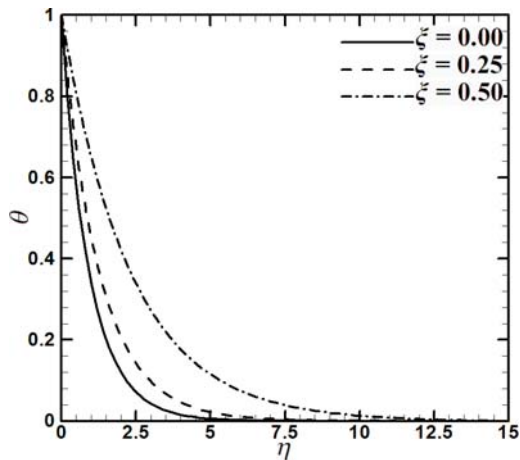


Fig. 17 Dimensionless temperature profiles for  $r = 1.00$  in negative inclination case

#### 4. Conclusions

1. The boundary layer solution of natural convective heat transfer along an inclined arbitrarily flat plate embedded in a saturated porous medium was presented. The wall temperature is power function of distance from the leading edge.

2. The solution was obtained by using the inclination parameter defined by Pop and Na [9] and defining a new coordinate system for both positive and negative inclinations of the plate. The numerical Keller box scheme implemented to discrete equations. The skin friction coefficient, Nusselt number, dimensionless velocity and temperature profiles were plotted for various values of  $r$  and  $\xi$ .

3. As it was observed in both of cases with increasing  $r$  at a fixed inclination angle, coefficient of skin friction and Nusselt number will increase. On the other hand, for positive inclination in  $\xi \approx 0.55$ , where longitudinal and normal components of buoyancy force are comparable, Nusselt number has a minimum. For negative inclination, the point where separation occurred was determined approximately. In this case, the Nusselt number decreased uniformly at a given  $r$  with increasing  $\xi$ .

4. Moreover there is a wonderful match between the numerical solution and similarity solutions for  $\xi = 0$  (horizontal plate) and  $\xi = 1$  (vertical plate), which are

presented by Cheng and Chang [14] and Cheng and Minkowycz [15] respectively.

#### References

1. **Nield, D.A.; Bejan, A.** 2006. Convection in Porous Media. 3rd ed. New York: Springer. 57p.
2. **Ingham, D.B.; Pop, I.** 2005. Transport Phenomena in Porous Media. 1st ed. Oxford: Elsevier Science. 60p.
3. **Vafai, K.** 2005. Handbook of Porous Media. 2nd ed. New York: Taylor and Francis. 201p.
4. **Pop, I.; Ingham, D.B.** 2001. Convective Heat Transfer: Mathematical and Computational Modelling of Viscous Fluids and Porous Media. Oxford: Pergamon. 375p.
5. **Ingham, D.B.; Bejan, A.; Mamut, E.; Pop, I.** 2004. Emerging Technologies and Techniques in Porous media. Dordrecht: Kluwer. 65p.
6. **Rees, D.A.S.; Riley, D.S.** 1985. Free convection above a near horizontal semi-infinite heated surface embedded in a saturated porous medium, *Int. J. Heat Mass Transfer*, vol.28: 183-190.
7. **Ingham, D.B.; Merkin, J.H.; Pop, I.** Natural convection from a semi-infinite flat plate inclined at a small angle to the horizontal in a saturated porous medium. *-Acta Mechanica*, 1985, vol. 57, p.185-202.
8. **Jang, J.Y.; Chang, W.J.** 1988. Buoyancy-induced inclined boundary layer flow in a saturated porous medium, *Comput. Methods Appl. Mech.*; vol.68: 333-344.
9. **Pop, I.; Na, T.Y.** 1996. Free convection from an arbitrarily inclined plate in a porous medium, *Heat Mass Transfer*, vol.32: 55-59.
10. **Hossain, M.A.; Pop, I.** 1997. Radiation effect on Darcy free convection flow along an inclined surface placed in porous media, *Heat Mass Transfer*, vol.32: 223-227.
11. **Vaszi, A.Z.; Ingham, D.B.; Lesnic, D.; Munslow, D.; Pop, I.** 2000. Conjugate free convection from a slightly inclined plate embedded in a porous medium, *Zeit. Angew. Math. Mech.*, vol.81: 465-479.
12. **Lesnic, D.; Ingham, D.B.; Pop, I.; Storr, C.** 2004. Free convection boundary layer flow above a nearly horizontal surface in a porous medium with Newtonian heating, *Heat Mass Transfer*, vol.40: 665-672.
13. **Keller, H.B.** 1978. Numerical methods in boundary layer theory, *Ann. Rev. Fluid Mech.*, vol.10: 417-433.
14. **Cheng, P.; Chang, I.D.** 1976. Buoyancy induced flows in a saturated porous medium adjacent to impermeable horizontal surfaces, *Heat Mass Transfer*, vol.19: 1267-1272.
15. **Cheng, P.; Minkowycz, W.J.** 1977. Free convection about a vertical flat plate embedded in a porous medium with application to heat transfer from a dike, *J. Geophys. Res.*, vol.82: 2040-2044.
16. **Cebeci, T.; Shao, J.P.; Kafeyke, F. Laurendeau, E.** 2005. Computational Fluid Dynamics for Engineers. Horizons Publishing: Springer.

M. H. Kayhani, E. Khaje, M. Sadi

PORINGOJE APLINKOJE FORMUOJAMŲ PASIENIO  
SLUOKSNIŲ NATŪRALIOJI KONVEKCIJA IŠILGAI  
NEPRALAIŽIŲ NUOŽULNIŲ PAVIRŠIŲ

R e z i u m ė

Tyrinėtas natūralus ribinių sluoksnių konvekcinis tekėjimas laisvai pasvirusioje plokštėje prisotintoje porėtoje aplinkoje, kur sienelės temperatūra yra atstumo nuo kreipiamosios briaunos laipsninė funkcija. Keliamajai jėgai nustatyti pritaikyta Darcy-Boussinesko aproksimacija. Kad visus horizontalių, pasvirusių ir vertikalų plokščių atvejus būtų galima išreikšti viena transformuota ribinių sluoksnių lygčių sistema, panaudotas pasvirimo parametras  $\zeta$ . Nelinijinės priklausomos parabolinės lygybės buvo išspręstos pagal žinomą baigtinių skirtumų schemą, esant teigiamam ir neigiamam plokštės posvyriui. Lygybių panašumas horizontaliųjų ir vertikalųjų plokščių ribiniams atvejams pasiektas atitinkamai laikant, kad  $\zeta = 0$  ir  $\zeta = 1$ . Detalūs paviršiaus trinties koeficientai ir Nussett skaičiai tiek bedimensiam greičiui, esant tiek temperatūros profiliams, yra nustatyti plačiam parametro  $\zeta$  diapazonui. Gauti rezultatai gerai sutapo su kituose straipsniuose paskelbtais rezultatais.

M. H. Kayhani, E. Khaje, M. Sadi

NATURAL CONVECTION BOUNDARY LAYER  
ALONG IMPERMEABLE INCLINED SURFACES  
EMBEDDED IN POROUS MEDIUM

S u m m a r y

The natural convection boundary layer flow on an arbitrarily inclined plate in a saturated porous medium is considered, where wall temperature is power function of the distance from the leading edge. Darcy-Boussinesq approximation is adopted to account for buoyancy force. Inclination parameter  $\zeta$  is used such that all cases of the horizontal, Inclined and vertical plates can be described by a single set of transformed boundary layer equations. The non-linear coupled parabolic equations have been solved

numerically by using an implicit finite-difference scheme for both positive and negative inclinations of the plate. Also, the similarity equations for the limiting cases of the horizontal and vertical plates are recovered by setting  $\zeta = 0$  and  $\zeta = 1$ , respectively. Detailed results for skin friction coefficient and Nusselt number as well as for dimensionless velocity and temperature profiles are presented for a wide range of the parameter  $\zeta$ . The comparison with other validated articles shows excellent agreement.

M. X. Kaixhani, E. Khaie, M. Sadi

ЕСТЕСТВЕННАЯ КОНВЕКЦИЯ ПРЕДЕЛЬНЫХ  
СЛОЕВ ЗАКРЕПЛЕННЫХ В ПОРИСТОЙ СРЕДЕ  
ВДОЛЬ НЕПРОНИЦАЕМЫХ НАКЛОННЫХ  
ПОВЕРХНОСТЕЙ

Р е з ю м е

Исследована естественная конвекция течения предельных слоев в свободно наклоненной пластине в насыщенной пористой среде, где температура стенки является степенной функцией расстояния от направляющей грани. Для определения несущей силы применена аппроксимация Данци-Боуссинеска. Использован такой параметр наклона  $\zeta$ , чтобы все случаи горизонтальных, наклонных и вертикальных пластин описывались одной трансформированной системой уравнений предельных слоев. Нелинейные зависимые параболические уравнения решены используя известную схему конечных разностей с положительным и отрицательным наклоном плоскости. Подобие уравнений в предельных случаях для горизонтальных и вертикальных пластин получено при использовании соответственно  $\zeta = 0$  и  $\zeta = 1$ . Детальные значения коэффициентов поверхностного трения и Нуссетт числа как для бездиффузионной скорости, так и профилей температуры определены для широкого диапазона параметра  $\zeta$ . Сопоставление результатов с результатами, опубликованными в других статьях, показало отличное их совпадение.

Received August 31, 2010

Accepted January 17, 2011